

Dissipative dynamics in quasifission

V. E. Oberacker,¹ A. S. Umar,¹ and C. Simenel²¹*Department of Physics and Astronomy, Vanderbilt University, Nashville, Tennessee 37235, USA*²*Department of Nuclear Physics, RSPE, Australian National University, Canberra, ACT 0200, Australia*

(Received 10 September 2014; published 10 November 2014)

Quasifission is the primary reaction mechanism that prevents the formation of superheavy elements in heavy-ion fusion experiments. Employing the time-dependent density functional theory approach, we study quasifission in the systems $^{40,48}\text{Ca}+^{238}\text{U}$. Results show that for ^{48}Ca projectiles the quasifission is substantially reduced in comparison to the ^{40}Ca case. This partly explains the success of superheavy element formation with ^{48}Ca beams. For the first time, we also calculate the repartition of excitation energies of the two fragments in a dynamic microscopic theory. The differences between both systems are interpreted in terms of initial neutron to proton asymmetry of the colliding partners.

DOI: [10.1103/PhysRevC.90.054605](https://doi.org/10.1103/PhysRevC.90.054605)

PACS number(s): 21.60.Jz, 24.10.-i, 25.70.Jj, 27.90.+b

I. INTRODUCTION

The creation of new elements is one of the most novel and challenging research areas of nuclear physics. The discovery of a region of the nuclear chart that can sustain the so-called *superheavy elements* (SHE) has led to intense experimental activity resulting in the discovery and confirmation of elements with atomic numbers as large as $Z = 117$ [1–3]. The theoretically predicted *island of stability* in the SHE region of the nuclear chart is the result of new proton and neutron shell closures, whose location is not precisely known [4–6]. The experiments to discover these new elements are notoriously difficult, with production cross sections in picobarns. Of primary importance for the experimental investigations is the choice of target-projectile combinations that have the highest probability for forming a compound nucleus that results in the production of the desired element. Experimentally, two approaches have been used for the synthesis of these elements, one utilizing doubly magic ^{208}Pb targets or ^{209}Bi (cold fusion) [7,8] and the other utilizing deformed actinide targets with neutron-rich projectiles (hot fusion), such as ^{48}Ca [1–3]. While both methods have been successful in synthesizing superheavy elements, the evaporation residue cross sections for hot fusion were found to be several orders of magnitude larger than those for cold fusion for the synthesis of the heaviest elements. To pinpoint the root of this difference it is important to understand the details of the reaction dynamics of these systems. For light- and medium-mass systems the capture cross section may be considered to be the same as that for complete fusion. For heavy systems leading to superheavy formations, however, the formation of a compound nucleus is dramatically reduced due to the quasifission (QF) process [9,10]. Consequently, quasifission is the primary reaction mechanism that limits the formation of superheavy nuclei. Quasifission is characterized by nuclear contact times that are usually greater than 5 zs but much shorter than typical fusion-fission times which require the formation of a compound nucleus [11–14].

Many experimental studies have been performed to understand the mechanisms at play in the quasifission process since its discovery [11–19]. Various theoretical models [20–22] have also been developed to help in the interpretation of these experimental data. These models are often based on statistical or

transport theories. In this paper, we consider another formalism based on a many-body quantum approach. We study quasifission with the fully microscopic time-dependent Hartree-Fock (TDHF) theory proposed by Dirac [23]. The TDHF theory provides a useful foundation for a fully microscopic many-body theory of large-amplitude collective motion. This approach has been widely applied to study heavy-ion collisions in nuclear physics [24,25]. The TDHF time evolution can correctly account for the heavy-ion interaction barriers [26–29] and thus reproduce the capture cross sections in heavy systems such as $^{48}\text{Ca}+^{238}\text{U}$ [29]. It is also able to describe transfer and deep-inelastic reactions [30–37] as well as the dynamics of fission fragments [38]. It is therefore a tool of choice to investigate quasifission mechanisms. However, the feasibility of using TDHF for quasifission has only been recognized recently [39]. These applications have been made possible thanks to considerable improvements of computational power in the past decade. Modern TDHF calculations are performed on a three-dimensional (3D) Cartesian grid with no symmetry restrictions and with much more accurate numerical methods [40–46].

II. METHODS

In the present TDHF calculations we use the Skyrme SLy4d energy density functional (EDF) [47], including all of the relevant time-odd terms in the mean-field Hamiltonian. First, we generate very accurate static HF wave functions for the two nuclei on the 3D grid. The initial separation of the two nuclei is 30 fm. In the second step, we apply a boost operator to the single-particle wave functions. The time propagation is carried out using a Taylor-series expansion (up to orders 10–12) of the unitary mean-field propagator, with a time step $\Delta t = 0.4 \text{ fm}/c$. Let us first focus on collisions of $^{40}\text{Ca}+^{238}\text{U}$. An example of a TDHF calculation for this reaction at $E_{\text{c.m.}} = 209 \text{ MeV}$ and an average orbital angular momentum quantum number $L = 20$ is shown in Fig. 1, where contour plots of the mass density are plotted at various times. In this case, the 3D lattice spans $(66 \times 56 \times 30) \text{ fm}$. As the nuclei approach each other, a neck forms between the two fragments which grows in size as the system begins to rotate. Due to the Coulomb repulsion

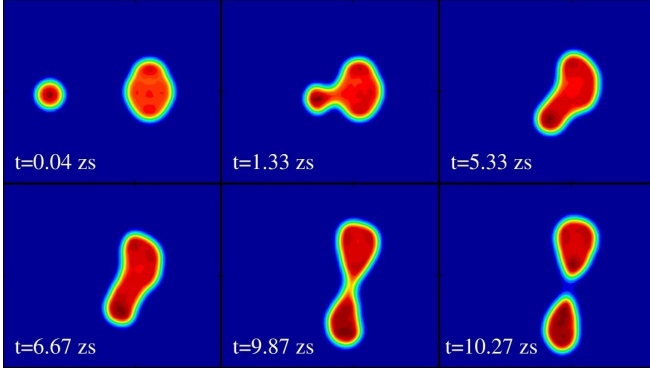


FIG. 1. (Color online) Quasifission in the reaction $^{40}\text{Ca}+^{238}\text{U}$ at $E_{c.m.} = 209$ MeV with impact parameter $b = 1.103$ fm ($L = 20$). Shown is a contour plot of the time evolution of the mass density.

and centrifugal forces, the dinuclear system elongates and forms a very long neck which eventually ruptures, leading to two separated fragments. The ^{238}U nucleus exhibits a strong quadrupole deformation. In the present study, its symmetry axis was oriented initially at 90° to the internuclear axis. For small impact parameters, this leads essentially to collisions with the side of ^{238}U . This orientation is also the one which leads to the largest “contact time” in central collisions [25,39]. We define the contact time as the time interval between the time t_1 when the two nuclear surfaces (defined as isodensities with half the saturation density $\rho_0/2 = 0.08$ fm $^{-3}$) first touch and the time t_2 when the dinuclear system splits up again. In the collision shown in Fig. 1, we find a contact time $\Delta t = 9.35$ zs and substantial mass transfer (66 nucleons to the light fragment). This contact time and mass transfer is characteristic for QF [12,14]. Collisions with the tip of ^{238}U may also result in QF, however, with smaller mass transfer. In addition, the latter orientations are never found to lead to fusion in TDHF calculations [25,39], which is consistent with experimental observation that fusion essentially occurs in collisions with the side of the deformed actinide target [15]. In this paper, our goal is to investigate QF reactions in competition with the formation of a compound nucleus by fusion. Therefore, we investigate only collisions with the side of ^{238}U .

III. RESULTS

Figure 2(a) displays the contact time as a function of the ratio of the center-of-mass energy $E_{c.m.}$ with the frozen Hartree-Fock barrier for central collisions ($L = 0$). This barrier is calculated for collisions with the side of ^{238}U [27]. Two fragments are always observed in the exit channel up to center-of-mass energies $\sim 10\%$ above the barrier. Globally, the contact time increases with energy and reaches a maximum of 32 zs at center-of-mass energy $\sim 10\%$ above the barrier. TDHF calculations carried out at higher energy ($E_{c.m.} \geq 223$ MeV) show *one* nucleus at the end of the calculation. In this case, contact times exceed 35 zs, which is interpreted as possible fusion reactions leading to the formation of a compound nucleus. The effect of a finite impact parameter b is to reduce this contact time as shown in Fig. 3(a). The above observations

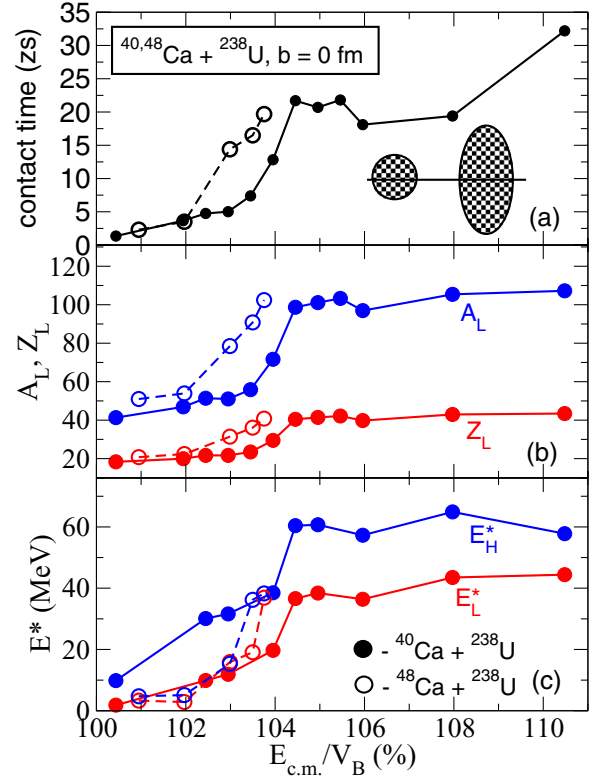


FIG. 2. (Color online) Several observables as a function of $E_{c.m.}/V_B$ for $^{40,48}\text{Ca}+^{238}\text{U}$ central collisions with the side of ^{238}U . The frozen HF barrier for these configurations are $V_B = 199.13$ MeV with ^{40}Ca and $V_B = 196.14$ MeV with ^{48}Ca . (a) Contact time, (b) mass and charge of the light fragment, and (c) excitation energy of the light and heavy fragments. Beyond the QF region only fusion is observed.

are consistent with the fact that contact time increases as matter overlap between the fragments at the distance of closest approach increases. However, we also observe a plateau at ~ 20 zs above $1.05V_B$ in Fig. 2(a) which cannot be explained with such simple considerations.

These contact times are long enough to enable the transfer of a large number of nucleons as shown in Fig. 2(b), where the masses A_L and charges Z_L of the light fragment are plotted. A plateau is again observed for energies of $\sim 5\text{--}10\%$ above V_B . This corresponds to a light fragment with $Z_L \simeq 40\text{--}42$ and $A_L \simeq 100\text{--}107$. Varying the impact parameter up to ~ 2 fm does not alter these observations as shown in Fig. 3(b). The root of this behavior may be due to the fact that Zr isotopes ($Z = 40$) in the mass range 100–112 are strongly bound with a large prolate deformation around $\beta_2 = 0.42$ [48–50]. Due to shell effects, these configurations may be energetically favorable during the QF dynamics [16,17,19]. A similar effect is observed in TDHF calculations of collisions with the tip of ^{238}U which favors the formation of fragments in the vicinity of the doubly magic ^{208}Pb nucleus [39].

The quasifission contact times are also long enough to enable the conversion of the initial relative kinetic energy into internal excitations. Experimentally, the measured total kinetic energy (TKE) of the quasifission fragments in $^{40,48}\text{Ca}+^{238}\text{U}$ reactions is in relatively good agreement with the Viola

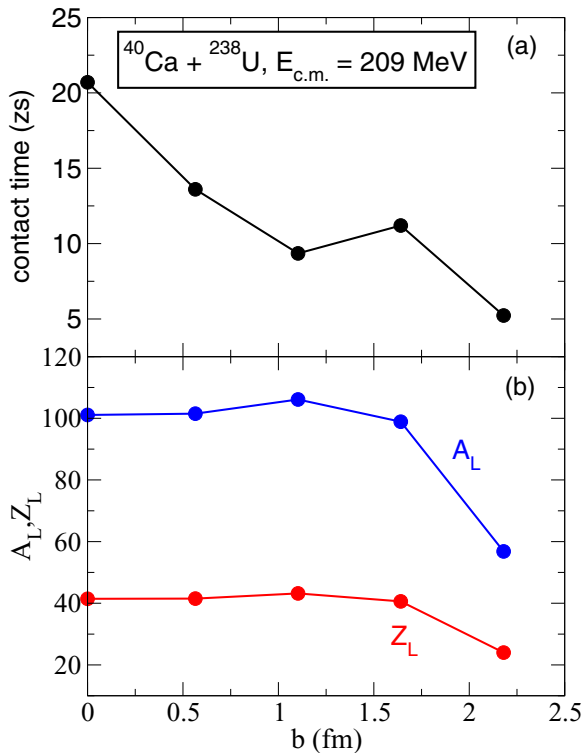


FIG. 3. (Color online) (a) Contact time and (b) mass and charge of the light fragment as a function of impact parameter.

systematics [12,18]. The TDHF approach contains one-body dissipation mechanisms which are dominant at near-barrier energy. It can then be used to predict the final TKE of the fragments. The TKE of the fragments formed in $^{40}\text{Ca}+^{238}\text{U}$ have been computed for a range of central collisions up to 10% above the barrier. Figure 4 shows that the TDHF predictions of TKE are in excellent agreement with the Viola systematics [51,52]. This indicates that the relative TKE of the quasifission fragments are primarily due to their Coulomb repulsion and do not carry a fraction of the initial TKE, as is the case for deep-inelastic collisions.

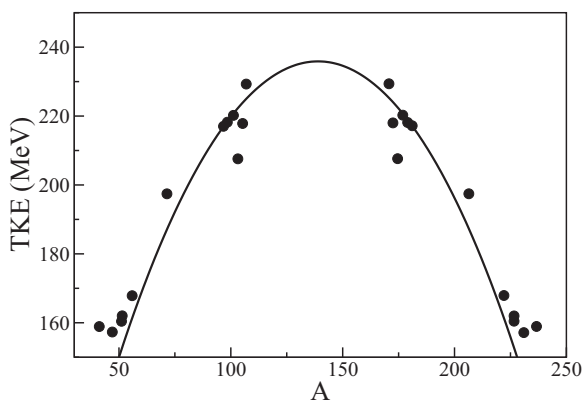


FIG. 4. TKE of both the light and heavy fragments formed in $^{40}\text{Ca}+^{238}\text{U}$ central collisions at $E_{c.m.}/V_B = 1.0-1.1$. The solid line represents TKE values based on the Viola formula [51].

The excitation energy and, in particular, its repartition between the fragments also provide important information on the dissipative nature of the reaction mechanisms [53–56]. Of course, in TDHF there is no thermalization in the true sense of the word, i.e., the TDHF does not change the entropy of the system. However, certainly TDHF involves so-called one-body dissipation, damping of collective energy with (nearly) random collisions of nucleons with the walls of the mean field. Recently, we have developed an extension to TDHF theory via the use of a density constraint to calculate fragment excitation energy of *each fragment* directly from the TDHF time evolution [57]. This gives us new information on the repartition of the excitation energy between the heavy and light fragments which is not available in standard TDHF calculations. In Fig. 2(c) we show the excitation energies of the light and heavy fragments. For $^{40}\text{Ca}+^{238}\text{U}$ at 5 to 10% above the barrier, we find excitation energies which are approximately constant with $E_H^{*(\text{TDHF})} \simeq 60$ MeV for the heavy fragment and $E_L^{*(\text{TDHF})} \simeq 40$ MeV for the light fragment, which seem to scale with the fragment masses as $E_i^{*(\text{eq})} \simeq E_{\text{tot}}^{*(\text{eq})} \frac{A_i}{A_{\text{tot}}}$. With total excitation energy $E_{\text{tot}}^{*(\text{eq})} \simeq 100$ MeV and fragment masses $A_L \simeq 100$ and $A_H \simeq 178$ [see Fig. 2(b)], this assumption would give $E_H^{*(\text{eq})} \simeq 64$ MeV and $E_L^{*(\text{eq})} \simeq 36$ MeV. This suggests that for $^{40}\text{Ca}+^{238}\text{U}$ central collisions dissipative mechanisms lead to sufficient randomization of the excitation energy among the internal degrees of freedom.

We have performed similar TDHF calculations for the more neutron-rich system $^{48}\text{Ca}+^{238}\text{U}$, with the purpose of investigating the role of neutron to proton ratio N/Z asymmetry of the colliding partners. Indeed, unlike ^{40}Ca ($N/Z = 1$), the more neutron-rich ^{48}Ca nucleus has an $N/Z = 1.4$, which is close to that of ^{238}U ($N/Z \simeq 1.6$). As shown in Figs. 2(a)–2(c), the TDHF predictions with ^{48}Ca dramatically differ as compared to the $^{40}\text{Ca}+^{238}\text{U}$ system: The quasifission region, as evidenced by long contact time and large mass transfer, is confined to a very narrow energy window with $E_{c.m.}/V_B \simeq 1.03-1.04$. Above these energies, large contact times exceeding 35 zs are found with ^{48}Ca . The threshold for fusion occurs then at much lower energy with ^{48}Ca than with ^{40}Ca .

This difference between both reactions could be due to the total neutron number and/or to the different initial N/Z asymmetries. Experimental investigations with similar projectiles at near-barrier energies have concluded that the variation of quasifission must be more strongly related to the properties in the entrance channel rather than properties of the composite system [58]. It has also been argued in the same work that the reduced quasifission with ^{48}Ca is due to the fact that it is a doubly magic nucleus and that it essentially keeps its magicity when it collides with a target of similar N/Z . Indeed, spherical shells are expected to result in “cold valleys” in the potential energy surface leading to the compact compound nuclei [59–61]. Fusion through these valleys may also be favored because energy dissipation should be weaker, allowing greater interpenetration before the initial kinetic energy is dissipated [62,63]. This last point is supported by the fact that both exit fragments have similar excitation energies in the $^{48}\text{Ca}+^{238}\text{U}$ reaction [see Fig. 2(c)]. Indeed, the fact

that E_i^* is not proportional to A_i indicates that the dissipative mechanisms were not able to randomize the excitation energy among all the internal degree of freedom. On the contrary, ^{40}Ca , which is also a doubly magic nucleus but with a smaller N/Z , encounters a rapid N/Z equilibration in the early stage of the collision, modifying its identity [56]. As a result, ^{40}Ca essentially behaves as a nonmagic nucleus, i.e., with more quasifission.

IV. CONCLUSION

In summary, we have done a comparative study of QF for the $^{40,48}\text{Ca}+^{238}\text{U}$ systems using microscopic TDHF theory. We see that the TKE of the QF fragments follow the Viola systematics with long contact time (up to ~ 30 zs) and large

mass transfer typical to QF. However, the $^{48}\text{Ca}+^{238}\text{U}$ system shows considerably less QF in comparison to the $^{40}\text{Ca}+^{238}\text{U}$ system. This elucidates the success of SHE synthesis with ^{48}Ca beams. The origin of the difference between both reactions is attributed to a longer survival of the magicity of ^{48}Ca in the collision process which reduces dissipation mechanisms. This scenario is supported by the new microscopic calculations of the division of the excitation energy between the fragments.

ACKNOWLEDGMENTS

We thank D. J. Hinde for useful discussion. This work has been supported by the U.S. Department of Energy under Grant No. DE-FG02-96ER40975 with Vanderbilt University and by the Australian Research Council Grant No. FT120100760.

-
- [1] Yu. Ts. Oganessian, F. Sh. Abdullin, P. D. Bailey, D. E. Benker, M. E. Bennett, S. N. Dmitriev, J. G. Ezold, J. H. Hamilton, R. A. Henderson, M. G. Itkis, Y. V. Lobanov, A. N. Mezentsev, K. J. Moody, S. L. Nelson, A. N. Polyakov, C. E. Porter, A. V. Ramayya, F. D. Riley, J. B. Roberto, M. A. Ryabinin, K. P. Rykaczewski, R. N. Sagaidak, D. A. Shaughnessy, I. V. Shirokovsky, M. A. Stoyer, V. G. Subbotin, R. Sudowe, A. M. Sukhov, Y. S. Tsyganov, V. K. Utyonkov, A. A. Voinov, G. K. Vostokin, and P. A. Wilk, *Phys. Rev. Lett.* **104**, 142502 (2010).
- [2] Y. T. Oganessian, F. S. Abdullin, C. Alexander, J. Binder, R. A. Boll, S. N. Dmitriev, J. Ezold, K. Felker, J. M. Gostic, R. K. Grzywacz, J. H. Hamilton, R. A. Henderson, M. G. Itkis, K. Miernik, D. Miller, K. J. Moody, A. N. Polyakov, A. V. Ramayya, J. B. Roberto, M. A. Ryabinin, K. P. Rykaczewski, R. N. Sagaidak, D. A. Shaughnessy, I. V. Shirokovsky, M. V. Shumeiko, M. A. Stoyer, N. J. Stoyer, V. G. Subbotin, A. M. Sukhov, Y. S. Tsyganov, V. K. Utyonkov, A. A. Voinov, and G. K. Vostokin, *Phys. Rev. Lett.* **109**, 162501 (2012).
- [3] J. Khuyagbaatar, A. Yakushev, C. E. Düllmann, D. Ackermann, L.-L. Andersson, M. Asai, M. Block, R. A. Boll, H. Brand, D. M. Cox, M. Dasgupta, X. Derks, A. Di Nitto, K. Eberhardt, J. Even, M. Evers, C. Fahlander, U. Forsberg, J. M. Gates, N. Gharibyan, P. Golubev, K. E. Gregorich, J. H. Hamilton, W. Hartmann, R.-D. Herzberg, F. P. Heßberger, D. J. Hinde, J. Hoffmann, R. Hollinger, A. Hübner, E. Jäger, B. Kindler, J. V. Kratz, J. Krier, N. Kurz, M. Laatiaoui, S. Lahiri, R. Lang, B. Lommel, M. Maiti, K. Miernik, S. Minami, A. Mistry, C. Mokry, H. Nitsche, J. P. Omtvedt, G. K. Pang, P. Papadakis, D. Renisch, J. Roberto, D. Rudolph, J. Runke, K. P. Rykaczewski, L. G. Sarmiento, M. Schädel, B. Schausten, A. Semchenkov, D. A. Shaughnessy, P. Steinegger, J. Steiner, E. E. Tereshatov, P. Thörle-Pospiech, K. Tinschert, T. Torres De Heidenreich, N. Trautmann, A. Türler, J. Uusitalo, D. E. Ward, M. Wegrzecki, N. Wiehl, S. M. Van Cleve, and V. Yakusheva, *Phys. Rev. Lett.* **112**, 172501 (2014).
- [4] M. Bender, K. Rutz, P.-G. Reinhard, J. A. Maruhn, and W. Greiner, *Phys. Rev. C* **60**, 034304 (1999).
- [5] A. Staszczak, A. Baran, and W. Nazarewicz, *Phys. Rev. C* **87**, 024320 (2013).
- [6] S. Ćwiok, P.-H. Heenen, and W. Nazarewicz, *Nature* **433**, 705 (2005).
- [7] S. Hofmann and G. Münzenberg, *Rev. Mod. Phys.* **72**, 733 (2000).
- [8] S. Hofmann, F. P. Heßberger, D. Ackermann, G. Münzenberg, S. Antalic, P. Cagarda, B. Kindler, J. Kojouharova, M. Leino, B. Lommel, R. Mann, A. G. Popeko, S. Reshitko, S. Šaro, J. Uusitalo, and A. V. Yeremin, *Eur. Phys. J. A* **14**, 147 (2002).
- [9] C.-C. Sahm, H.-G. Clerc, K.-H. Schmidt, W. Reisdorf, P. Armbruster, F. Heßberger, J. Keller, G. Münzenberg, and D. Vermeulen, *Z. Phys. A* **319**, 113 (1984).
- [10] K.-H. Schmidt and W. Morawek, *Rep. Prog. Phys.* **54**, 949 (1991).
- [11] R. Bock, Y. T. Chu, M. Dakowski, A. Gobbi, E. Grosse, A. Olmi, H. Sann, D. Schwalm, U. Lynen, W. Müller, S. Bjørnholm, H. Esbensen, W. Wölfl, and E. Morenzoni, *Nucl. Phys. A* **388**, 334 (1982).
- [12] J. Töke, R. Bock, G. Dai, A. Gobbi, S. Gralla, K. Hildenbrand, J. Kuzminski, W. Müller, A. Olmi, H. Stelzer, B. Back, and S. Bjørnholm, *Nucl. Phys. A* **440**, 327 (1985).
- [13] W. Q. Shen, J. Albinski, A. Gobbi, S. Gralla, K. D. Hildenbrand, N. Herrmann, J. Kuzminski, W. F. J. Müller, H. Stelzer, J. Töke, B. B. Back, S. Bjørnholm, and S. P. Sørensen, *Phys. Rev. C* **36**, 115 (1987).
- [14] R. du Rietz, E. Williams, D. J. Hinde, M. Dasgupta, M. Evers, C. J. Lin, D. H. Luong, C. Simenel, and A. Wakhle, *Phys. Rev. C* **88**, 054618 (2013).
- [15] D. J. Hinde, M. Dasgupta, J. R. Leigh, J. P. Lestone, J. C. Mein, C. R. Morton, J. O. Newton, and H. Timmers, *Phys. Rev. Lett.* **74**, 1295 (1995).
- [16] M. G. Itkis, J. Äystö, S. Beghini, A. Bogachev, L. Corradi, O. Dorvaux, A. Gadea, G. Giardina, F. Hanappe, I. Itkis, M. Jandel, J. Kliman, S. Khlebnikov, G. Kniajeva, N. Kondratiev, E. Kozulin, L. Krupa, A. Latina, T. Materna, G. Montagnoli, Y. Oganessian, I. Pokrovsky, E. Prokhorova, N. Rowley, V. Rubchenya, A. Rusanov, R. Sagaidak, F. Scarlassara, A. Stefanini, L. Stuttge, S. Szilner, M. Trotta, W. Trzaska, D. Vakhtin, A. Vinodkumar, V. Voskressenski, and V. Zagrebaev, *Nucl. Phys. A* **734**, 136 (2004).
- [17] K. Nishio, H. Ikezoe, S. Mitsuoka, I. Nishinaka, Y. Nagame, Y. Watanabe, T. Ohtsuki, K. Hirose, and S. Hofmann, *Phys. Rev. C* **77**, 064607 (2008).

- [18] K. Nishio, S. Mitsuoka, I. Nishinaka, H. Makii, Y. Wakabayashi, H. Ikezoe, K. Hirose, T. Ohtsuki, Y. Aritomo, and S. Hofmann, *Phys. Rev. C* **86**, 034608 (2012).
- [19] E. M. Kozulin, G. N. Knyazheva, S. N. Dmitriev, I. M. Itkis, M. G. Itkis, T. A. Loktev, K. V. Novikov, A. N. Baranov, W. H. Trzaska, E. Vardaci, S. Heinz, O. Beliuskina, and S. V. Khlebnikov, *Phys. Rev. C* **89**, 014614 (2014).
- [20] G. G. Adamian, N. V. Antonenko, and W. Scheid, *Phys. Rev. C* **68**, 034601 (2003).
- [21] Valery Zagrebaev and Walter Greiner, *J. Phys. G* **34**, 2265 (2007).
- [22] Y. Aritomo, *Phys. Rev. C* **80**, 064604 (2009).
- [23] P. A. M. Dirac, *Proc. Camb. Phil. Soc.* **26**, 376 (1930).
- [24] J. W. Negele, *Rev. Mod. Phys.* **54**, 913 (1982).
- [25] C. Simenel, *Eur. Phys. J. A* **48**, 152 (2012).
- [26] Kouhei Washiyama and Denis Lacroix, *Phys. Rev. C* **78**, 024610 (2008).
- [27] C. Simenel, M. Dasgupta, D. J. Hinde, and E. Williams, *Phys. Rev. C* **88**, 064604 (2013).
- [28] Lu Guo and Takashi Nakatsukasa, *EPJ Web Conf.* **38**, 09003 (2012).
- [29] A. S. Umar, V. E. Oberacker, J. A. Maruhn, and P.-G. Reinhard, *Phys. Rev. C* **81**, 064607 (2010).
- [30] A. S. Umar, V. E. Oberacker, and J. A. Maruhn, *Eur. Phys. J. A* **37**, 245 (2008).
- [31] Cédric Golabek and Cédric Simenel, *Phys. Rev. Lett.* **103**, 042701 (2009).
- [32] David J. Kedziora and Cédric Simenel, *Phys. Rev. C* **81**, 044613 (2010).
- [33] C. Simenel, *Phys. Rev. Lett.* **105**, 192701 (2010).
- [34] C. Simenel, *Phys. Rev. Lett.* **106**, 112502 (2011).
- [35] Kazuyuki Sekizawa and Kazuhiro Yabana, *Phys. Rev. C* **88**, 014614 (2013).
- [36] G. Scamps and D. Lacroix, *Phys. Rev. C* **87**, 014605 (2013).
- [37] D. Lacroix and S. Ayik, *Eur. Phys. J. A* **50**, 95 (2014).
- [38] C. Simenel and A. S. Umar, *Phys. Rev. C* **89**, 031601 (2014).
- [39] A. Wakhle, C. Simenel, D. J. Hinde, M. Dasgupta, M. Evers, D. H. Luong, R. du Rietz, and E. Williams, *Phys. Rev. Lett.* **113**, 182502 (2014).
- [40] C. Bottcher, M. R. Strayer, A. S. Umar, and P.-G. Reinhard, *Phys. Rev. A* **40**, 4182 (1989).
- [41] P.-G. Reinhard, A. S. Umar, K. T. R. Davies, M. R. Strayer, and S. J. Lee, *Phys. Rev. C* **37**, 1026 (1988).
- [42] A. S. Umar, M. R. Strayer, P.-G. Reinhard, K. T. R. Davies, and S.-J. Lee, *Phys. Rev. C* **40**, 706 (1989).
- [43] A. S. Umar, M. R. Strayer, J. S. Wu, D. J. Dean, and M. C. Güçlü, *Phys. Rev. C* **44**, 2512 (1991).
- [44] A. S. Umar and V. E. Oberacker, *Phys. Rev. C* **71**, 034314 (2005).
- [45] A. S. Umar and V. E. Oberacker, *Phys. Rev. C* **73**, 054607 (2006).
- [46] J. A. Maruhn, P.-G. Reinhard, P. D. Stevenson, and A. S. Umar, *Comp. Phys. Comm.* **185**, 2195 (2014).
- [47] Ka-Hae Kim, Takaharu Otsuka, and Paul Bonche, *J. Phys. G* **23**, 1267 (1997).
- [48] G. A. Lalazissis, S. Raman, and P. Ring, *At. Data Nucl. Data Tables* **71**, 1 (1999).
- [49] A. Blazkiewicz, V. E. Oberacker, A. S. Umar, and M. Stoitsov, *Phys. Rev. C* **71**, 054321 (2005).
- [50] J. K. Hwang, A. V. Ramayya, J. H. Hamilton, Y. X. Luo, A. V. Daniel, G. M. Ter-Akopian, J. D. Cole, and S. J. Zhu, *Phys. Rev. C* **73**, 044316 (2006).
- [51] V. E. Viola, K. Kwiatkowski, and M. Walker, *Phys. Rev. C* **31**, 1550 (1985).
- [52] D. J. Hinde, D. Hilscher, H. Rossner, B. Gebauer, M. Lehmann, and M. Wilpert, *Phys. Rev. C* **45**, 1229 (1992).
- [53] J. Töke and W. U. Schroder, *Ann. Rev. Nucl. Part. Sci.* **42**, 401 (1992).
- [54] P. Klein, J. Kratz, M. Guber, H. Zimmermann, W. Brühle, W. Reisdorf, and M. Schädel, *Z. Phys. A* **357**, 193 (1997).
- [55] I. Nishinaka, Y. Nagame, H. Ikezoe, M. Tanikawa, Y. L. Zhao, K. Sueki, and H. Nakahara, *Phys. Rev. C* **70**, 014609 (2004).
- [56] K.-H. Schmidt and B. Jurado, *Phys. Rev. C* **83**, 061601 (2011).
- [57] A. S. Umar, V. E. Oberacker, J. A. Maruhn, and P.-G. Reinhard, *Phys. Rev. C* **80**, 041601 (2009).
- [58] C. Simenel, D. J. Hinde, R. du Rietz, M. Dasgupta, M. Evers, C. J. Lin, D. H. Luong, and A. Wakhle, *Phys. Lett. B* **710**, 607 (2012).
- [59] A. Sandulescu, R. Gupta, W. Scheid, and W. Greiner, *Phys. Lett. B* **60**, 225 (1976).
- [60] G. Fazio, G. Giardina, G. Mandaglio, R. Ruggeri, A. I. Muminov, A. K. Nasirov, Y. T. Oganessian, A. G. Popeko, R. N. Sagaidak, A. V. Yeremin, S. Hofmann, F. Hanappe, and C. Stodel, *Phys. Rev. C* **72**, 064614 (2005).
- [61] Y. Aritomo, M. Ohta, and F. Hanappe, *J. Phys. G* **32**, 2245 (2006).
- [62] D. Hinde and M. Dasgupta, *Phys. Lett. B* **622**, 23 (2005).
- [63] P. Armbruster, *Ann. Rev. Nucl. Part. Sci.* **50**, 411 (2000).